



Memory effect and dynamics in PEDOT:PSS-based actuators under DC voltage

Lauréline Seurre, Sofiane Ghenna, Héléne Arena, Caroline Soyer, Sébastien Grondel, Cedric Plesse, Giao Tran Minh Nguyen, Frederic Vidal, Eric Cattan

► To cite this version:

Lauréline Seurre, Sofiane Ghenna, Héléne Arena, Caroline Soyer, Sébastien Grondel, et al.. Memory effect and dynamics in PEDOT:PSS-based actuators under DC voltage. SPIE Smart Structures + Nondestructive Evaluation, Conference 11587 - Electroactive Polymer Actuators and Devices XXIII, EAPAD 2021, Mar 2021, Online, United States. pp.47, 10.1117/12.2582537 . hal-03197919

HAL Id: hal-03197919

<https://hal.science/hal-03197919>

Submitted on 13 Jul 2022

HAL is a multi-disciplinary open access archive for the deposit and dissemination of scientific research documents, whether they are published or not. The documents may come from teaching and research institutions in France or abroad, or from public or private research centers.

L'archive ouverte pluridisciplinaire **HAL**, est destinée au dépôt et à la diffusion de documents scientifiques de niveau recherche, publiés ou non, émanant des établissements d'enseignement et de recherche français ou étrangers, des laboratoires publics ou privés.



Distributed under a Creative Commons Attribution 4.0 International License

Memory effect and dynamics in PEDOT:PSS-based actuators under DC voltage

L. Seurre^{*a}, S. Ghenna^a, H. Aréna^a, C. Soyer^a, S Grondel^a, C. Plesse^b, G.T.M. Nguyen^b, F. Vidal^b, E. Cattani^a

^aUniv. Polytechnique Hauts-de-France, CNRS, Univ. Lille, Yncrea, Centrale Lille, UMR 8520 - IEMN, DOAE, F-59313 Valenciennes, France

^bLPPI, EA2528, Institut des Matériaux, Université de Cergy-Pontoise, 5 mail Gay Lussac, Neuville sur Oise, F-95031 Cergy Cedex, France.

ABSTRACT

Conducting polymers have interested many research groups as they exhibit a large strain in response to electrical stimulation, which is promising for materials used in MEMS. To date, these micro-actuators have very often been characterized by applying an AC voltage to extract the produced strains and forces. However, many applications require subjecting the actuators to an electrical voltage threshold for about 10 seconds or until several minutes. A micro-camera tracking the displacements of an object, the actuation of a cochlear implant during surgery, or the closing of micro-tweezers for manipulation objects are potential applications for which actuation is achieved by applying a DC voltage. In this way, the kinetics to reach the maximum strain are identified and compared. The application of a DC voltage to the conducting polymer-based micro-actuator for an extended period of time results in the emergence of a “memory effect”. In particular, the actuator does not return to its initial position promptly after a short-circuit. In addition, the electromechanical measurements conducted show that the deformation obtained depends on the DC voltage used for the previous actuation. The memory effect is directly related to the intrinsic operation of micro-actuator trilayers where the separator (NBR/PEO) is filled with an ionic liquid electrolyte that is involved during oxidation and reduction of the conductive polymer electrodes (PEDOT:PSS/PEO). An explanation of the physico-chemical phenomena involved will be proposed. These results are needful for the modeling and future control of these conjugated polymer micro-actuators integrated into microsystems devices for real-life applications.

Keywords: Electroactive polymer, electronically conducting polymer, memory effect, relaxation, DC voltage

1. INTRODUCTION

There is a growing interest in future soft micro-robotics, which requires the use of highly compliant, flexible, and good adaptable materials. A category of these micro-robots will be used as micro-tools to improve the precision of the surgeons' work or to explore the human body, provided the tools are contained within volumes of a few cubic millimeters. The development of new generations of flexible materials that can be used as micro actuators and micro sensors is therefore necessary. Ionic electroactive polymers are especially attractive owing to their striking characteristics, vital for medical applications, of low driving voltages and operation under ambient conditions. Various types of ionic electroactive polymers operating under low voltage conditions have been developed, including conducting polymers¹⁻⁸, ionic polymer-metal composites⁹⁻¹¹, bulky gel polymers¹²⁻¹⁵. However, very few of them were developed to be subsequently miniaturized using microelectronic fabrication technologies such as photolithography patterning, thin films deposition and plasma etching, with thicknesses less than a few microns equivalent to those of the rigid micro-actuators traditionally used for microsystems production^{16,17}. Soft microsystems, including high-performance thin flexible actuators and sensors, and integrated proximity electronics on a flexible base, are essential elements for future soft micro-robots. Very thin conducting polymer poly(3,4-ethylenedioxythiophene) (PEDOT) and more recently poly(3,4-ethylene dioxothiophene):poly(styrene sulfonate) (PEDOT:PSS) based-actuators have been integrated into soft micro-structures with gold remote contacts^{18,19}. They have also received significant attention because they exhibit large strains and forces with a driving voltage of less than 2 V.

* laureline.seurre@etu.uphf.fr; phone +33 3 20 19 79 50

To compare the different types of actuator devices, their electromechanical performances, among other things, have primarily been studied with a square alternating current. However, this is not usually the operating mode of the actuators involved in micro-robot applications. A direct current (DC) signal or a voltage set-point step is often tuned to obtain the desired position of the actuator. Their motions are not periodic and do not alternate over time, but they should remain in the same position for several seconds or minutes. Applications, for which a quasistatic voltage is necessary, include the displacement of a micro-camera on the tip of an endoscope, the actuation of a cochlear implant during surgery, or closing micro-tweezers for handling human tissue. These applications show the great potential of conducting polymer based-actuators, and understanding their working mechanisms under DC voltage is becoming increasingly important for developing and controlling microdevices. In this way, knowing the dynamics of the actuator under DC voltage to reach a strain difference (SD) or force setpoint is necessary to understand the phenomenon. This solicitation results in the onset of a residual strain difference (RSD) when the supply voltage is shut down, i.e. when the capacitor (actuator) is fully discharged. The dynamics under DC voltage depend heavily on the materials used in single, bi, or trilayers and on whether the measurements are made in solution or air. Extensive studies have been carried out on a polypyrrole matrix, in particular by *Otero et al.* on the current, charge, and strain dynamics after previously subjecting the polymer film to cathodic potentials for long periods of time. The interpretation given is that the polymeric structure can be compacted either by applying high cathodic potentials or by maintaining those potentials for long periods of time. In this sense, a good combination of potential and time allows the degree of structure closure to be improved without any decrease in electrical properties due to degradation processes^{20–23}. *Sendai et al.*²³ studied electrochemomechanical strain under tensile stress in polypyrrole films, and discussed the results in terms of the relaxation of the anisotropic strain and the memory effect introduced during creeping. The actuator dynamics is affected by memory effect described also in^{24,25} for polypyrrole matrix with pendant titanocene dichloride centers, by applying a combination of different experimental conditions. It has been established that both electroactive components of the film, the polymer matrix and the immobilized centers, contribute to the memory effects. The studies on dynamics with ionic polymer metal composites (IPMCs) trilayer actuators^{26–28} focus more on the back-relaxation effect: actuator under DC voltage that relaxes slowly back towards its initial shape instead of holding its bent state. In this case, maintaining a static position other than neutral due to hysteresis and creep is difficult²⁹, hindering their precise control.

To our knowledge, there is very little applicable data to map the behavioral dynamics of conducting polymer-based actuators when a DC voltage is applied for several minutes. The objective of this paper is to identify the time-dependent correspondence between the transient input DC voltage and the shape of the conducting polymer-based actuators, and propose some interpretations. First, the innovative method used to fabricate the extremely small trilayer actuators tested (with a thickness of 35 μm and a surface area of a few square millimeters) is explained, and their traditionally accepted mode of operation (redox process) is quickly reviewed. Then, the specific measuring protocol related to the need to apply electrical voltages successively with the same polarity is briefly described. No back-relaxation effect on the SD is observed for periods as long as 10 min under voltage. However, in this paper, the study focuses more on the dynamics of relaxation under a short-circuit. The RSD is described, the evolution of SD and RSD following a repeated applied voltage is analyzed, and a macroscopic explanation of the phenomenon is proposed.

2. MATERIAL AND METHODS

2.1 Material

Poly(ethylene glycol) methyl ether methacrylate (PEGM, $M_n = 500 \text{ g.mol}^{-1}$), poly(ethylene glycol) dimethacrylate (PEGDM, $M_n = 750 \text{ g.mol}^{-1}$), ammonium persulfate (APS, 98 %) and cyclohexanone (>99.8 %) were obtained from Sigma Aldrich and used as received. Poly(3,4-ethylenedioxythiophene) polystyrene sulfonate (PEDOT:PSS) aqueous solution (Clevios PH1000, solid content 1.0 – 1.3 wt%) was purchased from Heraeus Precious Metals GmbH & Co. Nitrile-butadiene rubber (NBR), initiator dicyclohexyl peroxydicarbonate (DCPD), and 1-ethyl-3-methylimidazolium bis(trifluoromethanesulfonyl)imide (EMImTFSI 99.9%) were used as supplied from LANXESS, Groupe Arnaud and Solvionic, respectively.

2.2 Micro-actuators fabrication

The trilayer actuators composed of a PEO-NBR ion storage membrane (ISM) sandwiched between two electroactive PEDOT:PSS-PEO layers were fabricated using the layer stacking method¹⁹. The PEDOT:PSS-PEO casting solutions were

obtained by mixing PEO (poly(ethylene oxide)) precursors (mPEG, methacrylic functionalized PEG) composed of 50 wt% PEGM and 50 wt% PEGDM as the monomer and the crosslinker, respectively, with an aqueous dispersion of PEDOT:PSS (40wt% with respect to the final electrode, i.e. 60wt% PEDOT:PSS, equivalent to 1.15 wt% solid content). APS was also added to the solution (3 wt% with respect to mPEG) as a radical initiator for the precursors. The solution was stirred until dissolution. The resulting solution was cast (0.05 ml.cm^{-2}) onto a glass slide and placed on a heating plate at 50°C , to evaporate the water. The ion storage membrane located between the two polymer electrodes is based on a semi-interpenetrating polymer network layer composed of a PEO network (50 wt%) and a linear NBR (50wt%). First, the NBR solution was prepared by dissolving NBR in cyclohexanone to obtain a concentration of 20 wt%. The PEO precursors, consisting of PEGDM (25 wt% with respect to the PEO network) and PEGM (75 wt% with respect to the PEO network) were added to the NBR solution and stirred for 30 min. The radical initiator DCPD, 3 wt% with respect to the PEO network, was then added to the solution. The final solution was stirred until complete homogenization, then degassed. During the next step, the reactive mixture was spin coated ($3000 \text{ rpm} - 1000 \text{ rpm/s} - 30 \text{ s}$) onto the first PEDOT:PSS-PEO electrode layer and pre-polymerized in a closed annealing chamber under continuous nitrogen flow for 45 min at 50°C , to initiate the formation of the PEO network. The second PEDOT:PSS-PEO electrode was fabricated on top of the PEDOT:PSS/PEO-NBR/PEO bilayer in the same way as the first electrode: new solutions were prepared, cast and solidified at 50°C by evaporating the water. The resulting trilayer actuators were then placed in a closed annealing chamber and the final heat treatment was carried out at 50°C for 3 h followed by post-curing at 80°C for 1h under a continuous nitrogen flow. The thicknesses of each PEDOT:PSS/PEO electrode and the NBR/PEO layer obtained were $6\mu\text{m}$ and $13 \mu\text{m}$, respectively. The trilayer structures were then micro-patterned as microbeams using laser cutting and measured between 5 mm and 6 mm in length (L), 1 mm and 1.43 mm wide (w), and $35 \pm 1 \mu\text{m}$ thick (h). The micro-actuator beams were then swollen in ionic liquid (IL) EMImTFSI for 72 h to incorporate the ions necessary for the redox process and to perform characterizations at a later stage. To simplify reading afterwards, the “micro-actuators” will be called “actuators”.

3. RESULTS AND DISCUSSION

3.1 Micro-actuator operation

Electronically conducting polymer-based actuators are able to store energy; therefore, they can be assimilated to capacitors. For a better understanding of the following discussion, this part reminds the operation work of these actuators.

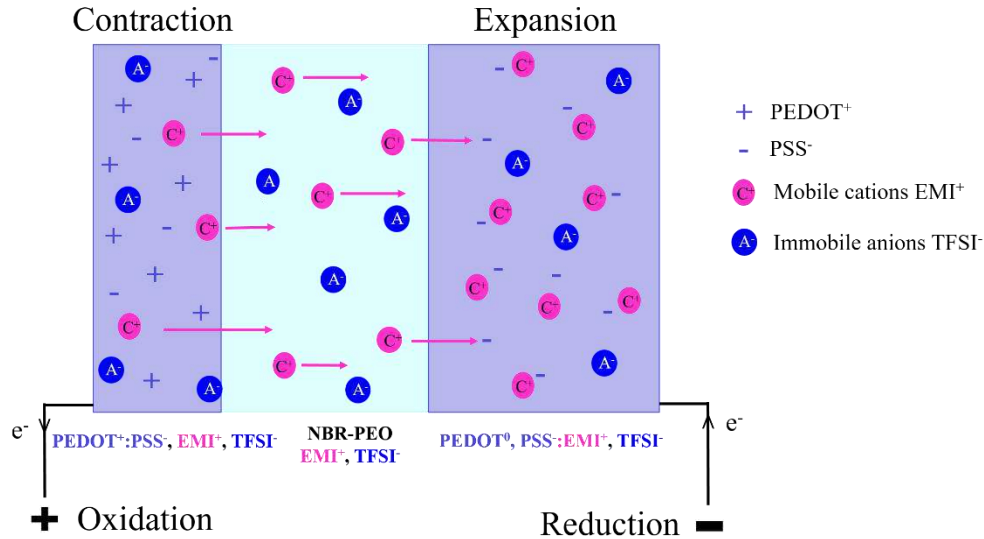
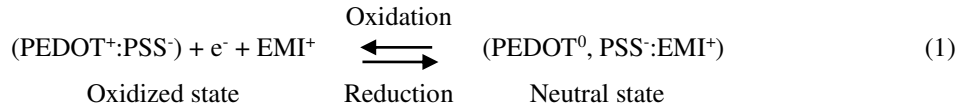


Figure 1: Schematic representation of the volume variation mechanism induced by the movement of ions in PEDOT:PSS-based trilayer actuators.

The principle of actuator operation is based on an oxidation-reduction process of the conductive polymer³⁰⁻³⁴, going from a doped state (removal of electrons, which corresponds to the oxidized state), to an undoped state (insertion of ions which

corresponds to the reduced state). The two conducting polymer layers successively undergo doping/undoping when they are electrically powered up. This electrochemical process, in both conducting polymer layers, leads to structural changes^{35–37}. In our case, the reduction of the p-doped conducting polymer lead to the dissociation of the polymer backbone (PEDOT⁰) with its counterion, PSS⁻. PSS⁻ is retained in the matrix because of its large size, which hinders its movement^{38,39}. Therefore, charge balancing is mainly achieved by the displacement of cations from the electrolyte (EMI⁺) in the PEDOT:PSS/PEO electrodes and in the NBR/PEO electrolyte support membrane between the two electrodes (Figure 1). The disappearance of positive charges on the PEDOT backbone makes the cations come into the cathode, while the appearance of positive charges on the PEDOT backbone at the anode makes the cations leave. When using IL, the electrochemical reactions leading to the expansion of one electrode during the reduction and simultaneously to the contraction of the other electrode during the oxidation are described by equation (1), and are responsible for the bending of the actuator:



The EMI⁺ are the mobile cations of the electrolyte governing actuation⁴⁰, and the TFSI⁻ are the immobile anions of the electrolyte, trapped between the chains of the PEDOT skeleton in the oxidized state, and therefore not participating in the reaction

3.2 Set-up and methods for characterization

To perform strain measurements, the actuator beams were hold between two glass plates covered with copper wires to apply the DC voltage. The maximum voltage was 1.75 V to avoid trilayer damage and it was decreased in 0.25 V increments from 1.75 V to 0.5 V. The experiments were performed from the side, in air, using a Dino Lite micro camera. The strain was recorded by measuring the curvature radius r of the beam on photos taken regularly. The radius length was obtained using three points along the edge of the beam.

The results were obtained by performing an electrical applied voltage for 10 min at each step. This duration was identified as allowing a level strain to be reached in all cases, i.e. the strain did not change by more than 0.1%/min of SD after 10 min to 20 min of applied voltage. After being switched on for 10 min, each actuator was short-circuited to discharge the charge accumulated by the capacitor, resulting in a peak current discharge lasting for a few seconds. The next measurement was carried out after 10 min of rest to give the beam time to return to its initial position. This time was defined as sufficient, as beyond this the relaxation strain reached a speed of 0.005%SD/min. Unless otherwise specified, this protocol was applied for the following measurements.

The strain difference (SD) is defined by h/r , where h is the thickness of the actuator. This study is focused on the actuator SD after applying an electrical voltage but also after switching off the electric voltage (short circuit). A particularity of the measurements presented is that the polarity remained unchanged when switching from one electrical voltage to another, the actuator is never subjected to an electrical voltage of reverse polarity. This situation is intended to simulate, for example, an actuator placed in a cochlear implant that must be deformed in a single direction to bend the implant in the cochlea as much as possible.

3.3 Dynamics of actuator strain under DC voltage

Figure 2b shows an untouched PEDOT:PSS-based actuator, before any electrical applied voltage. First actuation was achieved directly at 1.75 V and maintained for 10 min and a picture was taken to determine the actuator SD. During the first actuation, the PEDOT charges disappear at the cathode, making the cations of the IL move toward the cathode (Figure 1), while at the anode the appearance of positive charges on the PEDOT backbone makes the cations leave this electrode. It creates, in this case, an SD of 2.0% (Figure 2c). The conductive polymer electrodes were then immediately short-circuited. A new picture was taken after 10 min (Figure 2d) and a residual strain difference (RSD) of 0.6% was determined from the new radius of curvature, characterizing a beam that does not return to its initial vertical position. The actuator finds itself in unstable equilibrium position as, despite everything, it continues to move very slowly after the 10 min short-circuit as it will be seen later (Figure 3b). Immediately after this first measurement, a second measurement was carried out in the same way (Figure 2e&f). However, when this new measurement at 1.75 V began, the actuator was in the state of strain in Figure 2d (0.6%). The obtained total strain was 2.4% but the strain obtained between its initial and final position

was 1.8%, which is close to the value found during the first measurement (2.0%). Therefore, the actuator produces similar SDs under a same electrical voltage, but its final position in space is not the same. A new picture was taken after 10 min of short-circuit (Figure 2f) and a second residual strain difference (RSD2) of 0.97% was determined. The non-zero RSD (Figure 2d&f) indicates that the actuator memorizes part of the strain obtained under the previous voltage and that this memory effect is dependent on the accumulation of energy supplied to the actuator in the same direction of operation.

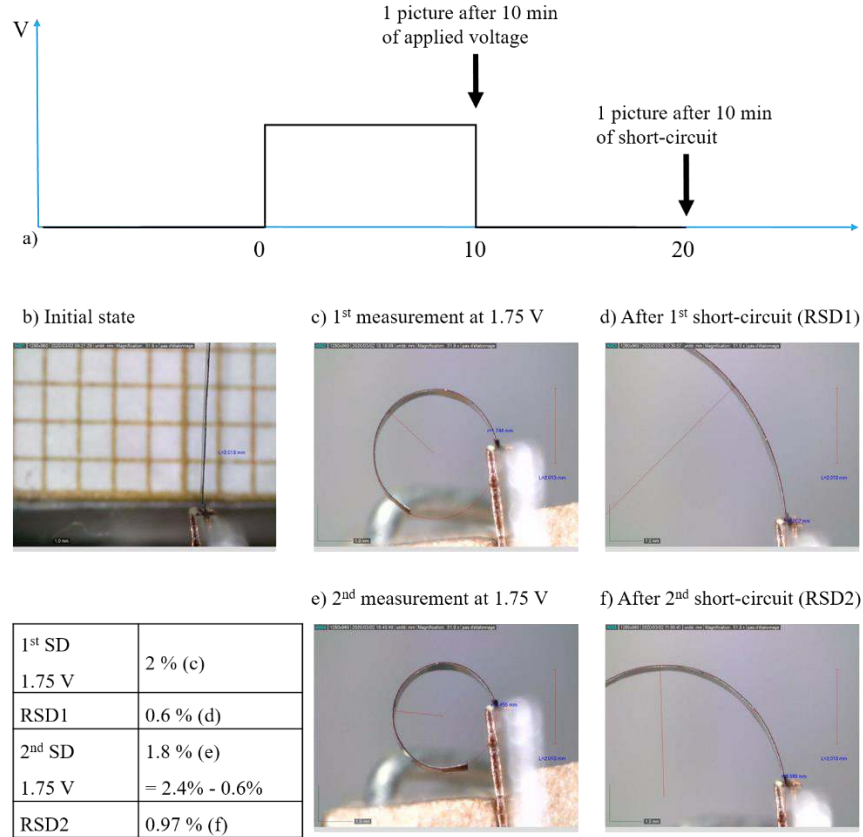


Figure 2: a) Chronovoltamogram of the measurement; b) PEDOT:PSS-based actuator in its initial state, before the first electrical connection; c) After application of a voltage of 1.75 V for 10 min; d) Picture taken of PEDOT:PSS electrodes after a short-circuit of 10 min to measure a residual strain difference (RSD1); e) Second application of a voltage of 1.75 V for 10min; f) Picture taken after a 10 min short-circuit to measure the residual strain difference (RSD2).

For an actuator that has not been powered up, it can be assumed that the ions of the IL are homogeneously distributed in the actuator. During the first applied voltage, electrons are removed from the PEDOT:PSS on the anode side (oxidation) and injected into the cathode side (reduction). The cations near the interface and in the ISM gradually move toward the ECP (the cathode), to compensate the disappearing of the positive charges on the reduced PEDOT backbone, while the cations in the anode are expelled toward the ISM due to the appearance of positive charges on the doped PEDOT backbone (Figure 1). The cations are then concentrated in or near the cathode. This concentration generates an increase in its volume, which causes spacing between the polymer chains of the ECP at the cathode, and the leaving of the cations at the anode generates its contraction, and thus the curvature of the whole actuator (Figure 2c&e). The cations are then subjected to a certain pressure that keep them concentrated in or near the cathode.

To better understand the influence of applied voltage on the RSD, the evolution of the RSD was recorded over 25 h, starting with short-circuit performed after a 10 min of actuation at 1.75 V (Figure 3b). This experiment provided us with the strain dynamics over a period longer than 10 min, which was compared to evolution of the RSD over time for a sample that had not been subjected to any voltage, having simply been mechanically deformed (Figure 3c).

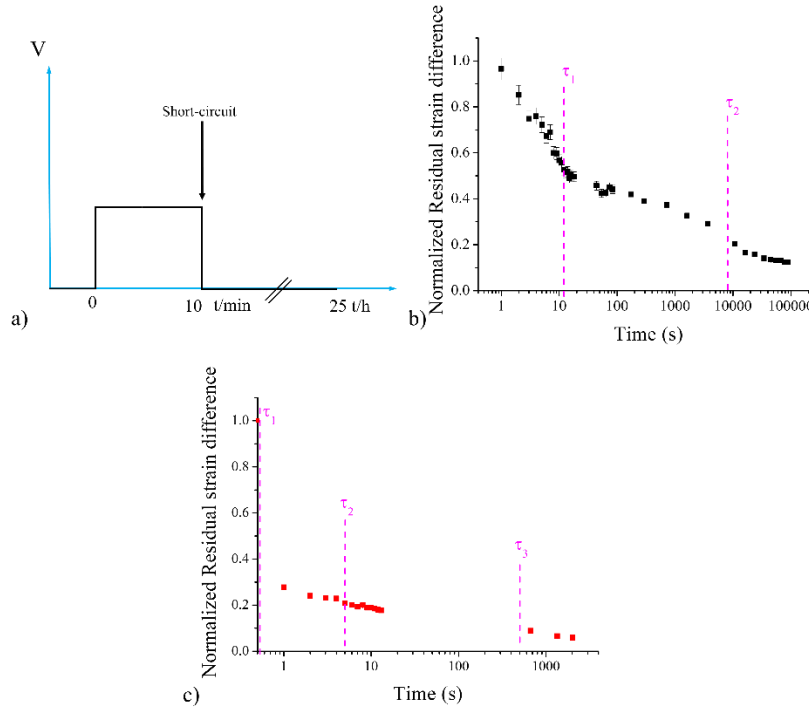


Figure 3: a) Chrono-voltamogram of a voltage supply followed by a short-circuit, and b) normalized (divided by the maximum value) RSD determined from the curvature radius as function of time after an applied voltage of 1.75 V for 10 min followed by short-circuit. The relaxation was recorded for 25 h. c) RSD of the purely mechanical relaxation of a beam containing IL recorded for 35 min: manual strain maintained for 10 min and then released.

To obtain this mechanical strain, the end of the actuator was bent around a cylindrical rod, to reproduce a strain similar to that obtained under electrical tension. This strain was maintained for 10 min, after which the locking system was removed and successive images were recorded for 35 min (Figure 3c). In this case, the RSD decreased sharply and reached zero in approximately 2000 s, indicating that the actuator had returned to its initial vertical position. Its relaxation dynamics can be described by three exponential decay functions, which correspond to a three phases relaxation: a first extremely fast phase with a constant time of only 0.3 s, a second slower phase with a constant time of 5 s, and a final even slower phase with a constant time of 524 s. 82% of the SD was lost in 13 s, and the beam returned to its initial vertical position after 30 min.

In the case of a relaxation after an applied voltage of 1.75 V (Figure 3b), even after 25 h the actuator had not returned to its vertical position. An unstable state was established and the actuator only returned to its initial vertical position after several days. Its relaxation dynamics followed a two decreasing exponential functions, corresponding to a fast relaxation with a constant time of $\tau_1 = 13$ s and a slower relaxation with a constant time of $\tau_2 = 7937$ s. The time required to lose 50% of the strain was 26 s, and in 4 h of relaxation the RSD reached 0.12%.

When a short-circuit is caused (actuator switching from the state in Figure 2c to the state in Figure 2d), a combination of at least two physical phenomena can be considered: (i) the reflux of the IL cations, and (ii) the purely mechanical relaxation of the beam.

- i. The short circuit enable the electrons in the ECP electrodes to flow out resulting in a current discharge peak. This charge movement causes the electrons to recombine on the polymer chains releasing the cations concentrated in or near the cathode³⁸. The cations flow back toward the ISM and the anode, changing the state of contraction and expansion of the two ECP electrodes and causing the beam to relax (Figure 2d&f, Figure 3b). As the cations are within a relatively dense matrix of polymer chains, they are located in an interstitial position between the polymer

chains. Therefore, they are slightly trapped and their limited mobility slows down the reflux. Consequently, as long as a reverse electrical voltage is not applied, the cations do not have enough energy to flow back quickly.

- ii. When a short circuit is caused, the beam releases the stored mechanical energy (viscoelasticity of the material). The ECP electrodes extended on one side and compressed on the other side, try to return to their initial position naturally by participating in the expulsion of the IL located between the polymer chains of the expanded cathode. The comparison of the curves in Figure 3b&c shows that the reflux of the IL ions slows the return of the actuator to the initial position: the constant time in the first phase of purely mechanical relaxation is only 0.3 s, i.e. 47 times faster than during relaxation following an electrical applied voltage and a short-circuit. In the last relaxation phase, the return to the initial position is slower in both situations, but purely mechanical relaxation is still 15 times faster. Therefore, in the first phase of relaxation (Figure 3b), the viscoelasticity of the material is the main contributor to the return of the microbeam to its initial position. This effect is then strongly slowed down by the IL reflux and then an unstable balance is established between the two phenomena. Only the presence of a high concentration of IL near and/or in the cathode can explain the maintenance of a curvature opposing the elastic strain of the beam, thus preserving part of the strain caused by the voltage applied to the beam.

When the actuator was subjected to a second applied voltage at 1.75 V, immediately after the previous 10 min short-circuit (Figure 2e), the total strain achieved relative to an initial vertical position was 2.4%. However, the final strain achieved takes into account the initial state of strain of the beam (RSD1 of 0.6% after the first measurement Figure 2d). When it is subtracted from the total strain, the SD becomes 1.8% (Figure 2). Therefore, a loss of 0.2% (2% to 1.8%) was observed after the second applied voltage. After the 10 min short-circuit, the RSD2 obtained was 0.97% (Figure 2f), which corresponds to a 0.37% increase in RSD compared to the previous RSD1. This repeated actuation (2×10 min) resulted in the accumulation of ions in the cathode. Even though the actuator still had a margin of strain, it had to fight against the difficulty of deforming the polymer (maximum elongation of the polymer chains) during the second actuation. This could explain why with the same energy, the SD obtained for the second actuation was slightly lower (by 0.2%). This problem of the mechanical strain limit of the structure is accentuated by the fact that during this second strain the actuator starts from an initial non-zero strain (0.6%, Figure 2d). Moreover, during the first application of an electric voltage, the mobility of the cations was better because they were moved over a "large" distance (from a state where the cations were homogeneously distributed in the actuator to a state where the cations were concentrated in the cathode). With the second applied voltage, the efficiency was lower because the cations had more limited mobility as they were already at the ISM/ECP interface or in the ECP. Conversely, the RSD was higher for the second measurement than for the first one indicating that the ion reflux was less efficient and that the concentration of IL remaining in or near the cathode was higher, thus maintaining the polymer chains in a swollen state at the cathode. This second applied voltage allowed more IL to be blocked between the polymer chains on the cathode side. Therefore, the unstable state of equilibrium, mentioned above is displaced spatially.

These results show that the total strain and the residual strain of the beam, under the applied voltage and time conditions described above, produced a positioning of the beam dependent on the prior distribution of the ions inside the actuator. Beyond a few minutes of actuation, the backflow of the IL following the short-circuit, disturbs the pure elastic mechanical return of the actuator, keeping it in a quasi-stable position and partially memorizing the action performed previously.

3.1 Strain difference and residual strain difference under various DC voltage

In the experiments described previously, the only electrical voltage applied was 1.75 V for periods of 10 min to deform the actuator. If such materials were used to actuate micro-robots, a succession of electrical solicitations with various voltage amplitudes and a return to zero between each measurement should be possible. This situation has therefore been taken into account to some extent in the measurements presented in Figure 4. A fresh actuator was used, that had never been electrically energized. Therefore, the initial distribution of ions inside this material was assumed to be homogeneous.

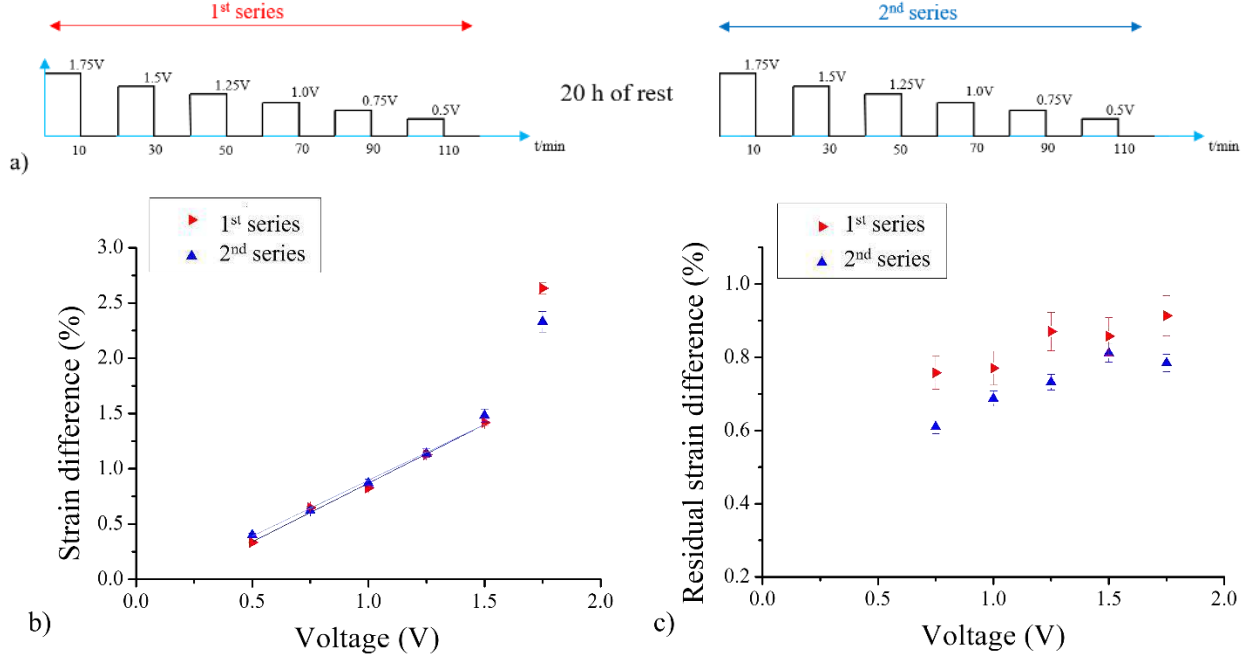


Figure 4: a) Chronovoltamogram of the two series of SD measurements. b) SD as function of decreasing applied voltage. c) RSD of the microbeam after a short-circuit as function of the applied voltage.

The experiment presented in Figure 4b started with a voltage of 1.75 V for 10 min, followed by a short circuit for 10 min, and this protocol was repeated by gradually decreasing the electrical voltage by 0.25 V, but always maintaining the same polarity (see chrono-voltamogram). The SD was calculated as described above, taking into account the RSD before actuation. A second series of SD measurements was performed on the same sample under the same conditions but after about 20 h of rest for the sample. This rest allowed time for part of the IL to be redistributed in the material and to reduce the RSD to around 0.1% (Figure 3b). For the two measurements (first and second series) conducted at a voltage of 1.75 V, it can be seen that the SD values differed by only 0.3% (Figure 4b) and are not on the axis as the line formed by the SD obtained for the other voltages (1.5 V to 0.5 V). These two SDs at 1.75 V, obtained for the initial states where the distribution of the IL was particularly homogeneous are different from the other SD values obtained at the lower electrical voltages (1.5 to 0.5 V). This result confirms the hypothesis described above, which indicates that if the cations distribution is initially homogeneous or has regained a certain homogeneity in the actuator due to resting the material, then the strain is amplified. The offset of 0.3% between the two SDs at 1.75V confirms the results in Figure 2b&d ($SD1b-SD1d = 0.2\%$). In our opinion, these effects are closely related to the dynamics of cation movement, which is favored when they are homogeneously or relatively homogeneously distributed in the material. Conversely, this dynamic is more limited when the cations are already concentrated in or near the cathode and when they have not had sufficient time to flow back. This is indeed what was observed for actuation at lower electrical voltages where the measurements were taken after 10 min of actuation (for SD) and 10 min of short-circuit (for RSD) and the operation was done for the next voltage right after. This does not allow sufficient time for the IL to flow back (10 min of short-circuit compared to 20 h) and results every time in a significant RSD varying between 0.6% and 0.9% (Figure 4c). The energy supplied then has the simple role of re-switching part of the cations that had flowed back during the period when the actuator was short-circuited. In the configuration where the cations remain close to the cathode, then the SD is proportional to the electrical voltage supplied. Figure 4b also shows that if the experiment is repeated under the same conditions after 20 h of rest, the SD was repeatable provided that the RSD before each electrical voltage applied was taken into account.

The RSDs measured after the short-circuits as a function of the various applied voltages are shown in Figure 4c. For both sets of measurements, a decrease in RSD was observed as the applied voltage decreased. This indicates that the actuator returns more easily to the vertical position as more electrical voltages are applied one after another. This was also confirmed by the lower RSDs of the second series compared to the first. The decrease in RSD with the successive application of

electrical voltages, which indicates that the beam returns to a position increasingly closer to vertical after a short circuit, could be explained by an increase in the mobility of the ions which is facilitated the more electrical voltages are applied.

4. CONCLUSION

In this paper, the strain and its dynamics of PEDOT:PSS polymer-based trilayer micro-actuators were studied. The measurements were carried out by applying a DC voltage for 10 min followed by a short circuit for 10 min before any other operation. The polarity was preserved between each measurement; only the amplitude of the signal was modified. The SD measured after applying a voltage for 10 min and the RSD measured after a 10 min short circuit were thoroughly analyzed. This study has highlighted the following points: (1) The purely mechanical relaxation of a micro-actuator is much faster than that of an actuator previously subjected to an electrical voltage and a short circuit; (2) In the latter situation the actuator returns to its vertical position after several days, but after 10 min an RSD could be measured for a relatively stable state of the micro-actuator; (3) The RSD observed indicates that the cations did not return to their original position after the short-circuit; and that after 10 min, the reflux of the ions was slow; (4) The overall SD obtained depends on the previous RSD. Then, the position of the beam in space, when it is energized, or after a short circuit, varies slightly depending on the previous states imposed on this beam; (5) The first electrical voltage applied to the actuator is more efficient than the subsequent ones, favored by a prior homogeneous cation distribution in the material; (6) Without time in standby, the SDs obtained successively evolve linearly with the voltages applied as long as the previous state of the beam (RSD) is taken into account; (7) The successive application of a DC electrical voltage with the same polarity promotes an increase in the mobility of the ions, characterized by a continuously decreasing RSD. These phenomena, which are directly related to the intrinsic operation of the actuator, are similar to a memory effect resulting from the combination of the distribution of the ions in the actuator and their low mobility.

ACKNOWLEDGMENTS

This work was supported by the H2020 project TWINNIMS (Grant agreement 857263), the French Government through the National Research Agency (ANR) and the MicroTIP, ROBOCOP, PIA EQUIPEX LEAF (ANR-11-EQPX-0025) projects, and the French RENATECH network.

REFERENCES

- [1] Baughman, R. H. Conducting polymer artificial muscles. *Synth. Met.* (1996). doi:10.1016/0379-6779(96)80158-5
- [2] Kaneto, K., Kaneko, M., Min, Y. & MacDiarmid, A. G. 'Artificial muscle': Electromechanical actuators using polyaniline films. *Synth. Met.* (1995). doi:10.1016/0379-6779(94)03226-V
- [3] Smela, E. Conjugated polymer actuators for biomedical applications. *Advanced Materials* (2003). doi:10.1002/adma.200390113
- [4] Plesse, C., Vidal, F., Teyssié, D. & Chevrot, C. Conducting polymer artificial muscle fibres: Toward an open air linear actuation. *Chem. Commun.* (2010). doi:10.1039/c001289k
- [5] Vidal, F., Plesse, C., Teyssié, D. & Chevrot, C. Long-life air working conducting semi-IPN/ionic liquid based actuator. *Synth. Met.* (2004). doi:10.1016/j.synthmet.2003.10.005
- [6] Khaldi, A. et al. Conducting interpenetrating polymer network sized to fabricate microactuators. *Appl. Phys. Lett.* (2011). doi:10.1063/1.3581893
- [7] Khaldi, A., Plesse, C., Vidal, F. & Smoukov, S. K. Smarter Actuator Design with Complementary and Synergetic Functions. *Adv. Mater.* (2015). doi:10.1002/adma.201500209
- [8] Maziz, A., Plesse, C., Soyer, C., Cattani, E. & Vidal, F. Top-down Approach for the Direct Synthesis, Patterning, and Operation of Artificial Micromuscles on Flexible Substrates. *ACS Appl. Mater. Interfaces* (2016). doi:10.1021/acsami.5b09577

- [9] Asaka, K., Oguro, K., Nishimura, Y., Mizuhata, M. & Takenaka, H. Bending of Polyelectrolyte Membrane-Platinum Composites by Electric Stimuli I. Response Characteristics to Various Waveforms. *Polym. J.* (1995). doi:10.1295/polymj.27.436
- [10] Nemat-Nasser, S. & Li, J. Y. Electromechanical response of ionic polymer-metal composites. *J. Appl. Phys.* (2000). doi:10.1063/1.372343
- [11] Tiwari, R. & Garcia, E. The state of understanding of ionic polymer metal composite architecture: A review. *Smart Materials and Structures* (2011). doi:10.1088/0964-1726/20/8/083001
- [12] Fukushima, T., Asaka, K., Kosaka, A. & Aida, T. Fully plastic actuator through layer-by-layer casting with ionic-liquid-based bucky gel. *Angew. Chemie - Int. Ed.* (2005). doi:10.1002/anie.200462318
- [13] Lee, J. & Aida, T. 'Bucky gels' for tailoring electroactive materials and devices: The composites of carbon materials with ionic liquids. *Chemical Communications* (2011). doi:10.1039/c1cc00043h
- [14] Asaka, K. et al. Highly conductive Sheets from Millimeter-Long Single-Walled carbon nanotubes and ionic liquids: Application to Fast-Moving, Low-Voltage electromechanical actuators operable in air. *Adv. Mater.* (2009). doi:10.1002/adma.200802817
- [15] Imaizumi, S., Kato, Y., Kokubo, H. & Watanabe, M. Driving mechanisms of ionic polymer actuators having electric double layer capacitor structures. *J. Phys. Chem. B* (2012). doi:10.1021/jp301501c
- [16] Smela, E., Inganäs, O. & Lundström, I. Controlled folding of micrometer-size structures. *Science* (80-.). (1995). doi:10.1126/science.268.5218.1735
- [17] Jager, E. W. H., Smela, E. & Inganäs, O. Microfabricating conjugated polymer actuators. *Science* (2000). doi:10.1126/science.290.5496.1540
- [18] Rohtlaid, K. et al. PEDOT:PSS-based micromuscles and microsensors fully integrated in flexible chips. *Smart Mater. Struct.* 29, 09LT01 (2020).
- [19] Seurre, L. et al. Demonstrating Full Integration Process for Electroactive Polymer Microtransducers to Realize Soft Microchips. in *Proceedings of the IEEE International Conference on Micro Electro Mechanical Systems (MEMS)* (2020). doi:10.1109/MEMS46641.2020.9056371
- [20] Grande, H. & Otero, T. F. Conformational movements explain logarithmic relaxation in conducting polymers. *Electrochim. Acta* (1999). doi:10.1016/S0013-4686(98)00298-9
- [21] Grande, H. & Otero, T. F. Intrinsic asymmetry, hysteresis, and conformational relaxation during redox switching in polypyrrole: A coulometric study. *J. Phys. Chem. B* (1998). doi:10.1021/jp9815356
- [22] Otero, T. F., Grande, H. J. & Rodríguez, J. Reinterpretation of polypyrrole electrochemistry after consideration of conformational relaxation processes. *J. Phys. Chem. B* (1997). doi:10.1021/jp9630277
- [23] Sendai, T., Suematsu, H. & Kaneto, K. Anisotropic strain and memory effect in electrochemomechanical strain of polypyrrole films under high tensile stresses. *Jpn. J. Appl. Phys.* (2009). doi:10.1143/JJAP.48.051506
- [24] Yamaura, M., Sato, K., Hagiwara, T. & Iwata, K. Memory effect of electrical conductivity upon the counteranion exchange of polypyrrole films. *Synth. Met.* (1992). doi:10.1016/0379-6779(92)90237-D
- [25] Vorotyntsev, M. A., Skompska, M., Pousson, E., Goux, J. & Moise, C. Memory effects in functionalized conducting polymer films: Titanocene derivatized polypyrrole in contact with THF solutions. *J. Electroanal. Chem.* (2003). doi:10.1016/S0022-0728(03)00038-X
- [26] Porfiri, M., Leroni, A. & Bardella, L. An alternative explanation of back-relaxation in ionic polymer metal composites. *Extrem. Mech. Lett.* (2017). doi:10.1016/j.eml.2017.01.009
- [27] Vunder, V., Punning, A. & Aabloo, A. Mechanical interpretation of back-relaxation of ionic electroactive polymer actuators. *Smart Mater. Struct.* (2012). doi:10.1088/0964-1726/21/11/115023
- [28] Liu, Y. et al. Ion transport and storage of ionic liquids in ionic polymer conductor network composites. *Appl. Phys. Lett.* (2010). doi:10.1063/1.3432664
- [29] Jo, C., Pugal, D., Oh, I. K., Kim, K. J. & Asaka, K. Recent advances in ionic polymer-metal composite actuators and their modeling and applications. *Progress in Polymer Science* (2013). doi:10.1016/j.progpolymsci.2013.04.003
- [30] Otero, T. F., Martinez, J. G. & Arias-Pardilla, J. Biomimetic electrochemistry from conducting polymers. A review. *Electrochim. Acta* (2012). doi:10.1016/j.electacta.2012.03.097
- [31] Otero, T. F. Biomimetic conducting polymers: Synthesis, materials, properties, functions, and devices. *Polymer Reviews* (2013). doi:10.1080/15583724.2013.805772
- [32] De Rossi, D. & Chiarelli, P. Biomimetic Macromolecular Actuators. in (1993). doi:10.1021/bk-1994-0548.ch040
- [33] Pei, Q. & Inganäs, O. Electrochemical applications of the bending beam method; a novel way to study ion transport in electroactive polymers. *Solid State Ionics* (1993). doi:10.1016/0167-2738(93)90291-A

- [34] Otero, T. F., Angulo, E., Rodríguez, J. & Santamaría, C. Electrochemomechanical properties from a bilayer: polypyrrole / non-conducting and flexible material - artificial muscle. *J. Electroanal. Chem.* (1992). doi:10.1016/0022-0728(92)80495-P
- [35] Otero, T. F. & Martinez, J. G. Electro-chemo-biomimetics from conducting polymers: Fundamentals, materials, properties and devices. *Journal of Materials Chemistry B* (2016). doi:10.1039/c6tb00060f
- [36] Ouyang, J., Chu, C. W., Chen, F. C., Xu, Q. & Yang, Y. High-conductivity poly(3,4-ethylenedioxythiophene):poly(styrene sulfonate) film and its application in polymer optoelectronic devices. *Adv. Funct. Mater.* (2005). doi:10.1002/adfm.200400016
- [37] Ouyang, J. et al. On the mechanism of conductivity enhancement in poly(3,4-ethylenedioxythiophene):poly(styrene sulfonate) film through solvent treatment. *Polymer (Guildf)*. (2004). doi:10.1016/j.polymer.2004.10.001
- [38] Löffler, S., Libberton, B. & Richter-Dahlfors, A. Organic bioelectronic tools for biomedical applications. *Electronics (Switzerland)* (2015). doi:10.3390/electronics4040879
- [39] Park, H. S., Ko, S. J., Park, J. S., Kim, J. Y. & Song, H. K. Redox-active charge carriers of conducting polymers as a tuner of conductivity and its potential window. *Sci. Rep.* (2013). doi:10.1038/srep02454
- [40] David, M. Applications of ionic liquids in polymer science and technology. *Applications of Ionic Liquids in Polymer Science and Technology* (2015). doi:10.1007/978-3-662-44903-5